UNIVERSITY^{OF} BIRMINGHAM

University of Birmingham Research at Birmingham

Cortical oscillatory mechanisms supporting the control of human social-emotional actions

Bramson, B.; Jensen, Ole; Toni, I.; Roelofs, K.

DOI:

10.1523/JNEUROSCI.3382-17.2018

License:

None: All rights reserved

Document Version
Peer reviewed version

Citation for published version (Harvard):

Bramson, B, Jensen, O, Toni, I & Roelófs, K 2018, 'Cortical oscillatory mechanisms supporting the control of human social-emotional actions', *The Journal of Neuroscience*, vol. 38, no. 25, pp. 3382-3417. https://doi.org/10.1523/JNEUROSCI.3382-17.2018

Link to publication on Research at Birmingham portal

Publisher Rights Statement:

Copyright © 2018 Society of Neuroscience.

General rights

Unless a licence is specified above, all rights (including copyright and moral rights) in this document are retained by the authors and/or the copyright holders. The express permission of the copyright holder must be obtained for any use of this material other than for purposes permitted by law.

•Users may freely distribute the URL that is used to identify this publication.

•Users may download and/or print one copy of the publication from the University of Birmingham research portal for the purpose of private study or non-commercial research.

•User may use extracts from the document in line with the concept of 'fair dealing' under the Copyright, Designs and Patents Act 1988 (?)

•Users may not further distribute the material nor use it for the purposes of commercial gain.

Where a licence is displayed above, please note the terms and conditions of the licence govern your use of this document.

When citing, please reference the published version.

Take down policy

While the University of Birmingham exercises care and attention in making items available there are rare occasions when an item has been uploaded in error or has been deemed to be commercially or otherwise sensitive.

If you believe that this is the case for this document, please contact UBIRA@lists.bham.ac.uk providing details and we will remove access to the work immediately and investigate.

Download date: 20. Mar. 2024

This Accepted Manuscript has not been copyedited and formatted. The final version may differ from this version.



Research Articles: Behavioral/Cognitive

Cortical oscillatory mechanisms supporting the control of human socialemotional actions

Bob Bramson¹, Ole Jensen², Ivan Toni¹ and Karin Roelofs^{1,3}

¹Donders Institute for Brain, Cognition and Behaviour, Centre for Cognitive Neuroimaging, Radboud University Nijmegen, 6525 EN Nijmegen, The Netherlands

DOI: 10.1523/JNEUROSCI.3382-17.2018

Received: 27 November 2017

Revised: 17 April 2018

Accepted: 11 May 2018

Published: 23 May 2018

Author contributions: B.B., O.J., I.T., and K.R. designed research; B.B. performed research; B.B. analyzed data; B.B., O.J., I.T., and K.R. wrote the paper.

Conflict of Interest: The authors declare no competing financial interests.

This work was supported by a starting grant from European Research Council (Grant ERC_StG2012_313749) awarded to K.R.

Correspondence: Bob Bramson, Donders Centre for Cognitive Neuroimaging, Radboud University Nijmegen, Trigon Building, Kapittelweg 29, 6525 EN Nijmegen, The Netherlands, Phone: +31(0)24 3622400, E-mail: b.bramson@donders.ru.nl

Cite as: J. Neurosci; 10.1523/JNEUROSCI.3382-17.2018

Alerts: Sign up at www.jneurosci.org/cgi/alerts to receive customized email alerts when the fully formatted version of this article is published.

Accepted manuscripts are peer-reviewed but have not been through the copyediting, formatting, or proofreading process.

²School of Psychology, University of Birmingham, B152TT Birmingham, UK

³Behavioural Science Institute (BSI), Radboud University Nijmegen, 6525 HR Nijmegen, The Netherlands

| 1 | Cortical oscillatory mechanisms supporting the control of human social-emotional actions |
|----------|--|
| 2 | Bob Bramson ¹ , Ole Jensen ² , Ivan Toni ^{1,*} and Karin Roelofs ^{1,3,*} |
| 3 | |
| 4 | ¹ Donders Institute for Brain, Cognition and Behaviour, Centre for Cognitive Neuroimaging, Radbour |
| 5 | University Nijmegen, 6525 EN Nijmegen, The Netherlands |
| 6 | ² School of Psychology, University of Birmingham, B15 2TT Birmingham, UK |
| 7 | ³ Behavioural Science Institute (BSI), Radboud University Nijmegen, 6525 HR Nijmegen, The |
| 8 | Netherlands |
| 9 | *These authors contributed equally. |
| 10 | |
| 11 | Abbreviated title: Controlling social-emotional actions |
| 12 | Conflicts declared: none. |
| 13 | |
| 14 | Acknowledgements: This work was supported by a starting grant from European Research Council |
| 15 16 | (Grant ERC_StG2012_313749) awarded to K.R. |
| 17 | Number of pages: 28 |
| 18 | Number of figures: 5 |
| 19 | Words abstract: 248 |
| 20 | Words significance statement: 112 |
| 21 | Words introduction: 644 |
| 22 | Words discussion: 1499 |
| 23 | |
| 24 | Correspondence: |
| 25 | Bob Bramson |
| 26 | Donders Centre for Cognitive Neuroimaging |
| 27 | Radboud University Nijmegen |
| 28 | Trigon Building Kapittelweg 29 |
| 29 30 | 6525 EN Nijmegen |
| 31 | The Netherlands |
| 32 | Phone: +31(0)24 3622400 |
| 33 | E-mail: b.bramson@donders.ru.nl |
| 34 | |
| 35 | |

Abstract

The human anterior prefrontal cortex (aPFC) is involved in regulating social-emotional behavior, presumably by modulating effective connectivity with down-stream parietal, limbic, and motor cortices. Regulating that connectivity might rely on theta-band oscillations (4-8 Hz), a brain rhythm known to create overlapping periods of excitability between distant regions by temporally releasing neurons from inhibition. Here, we use magnetoencephalography (MEG) to understand how aPFC theta-band oscillations implement control over prepotent social-emotional behaviors, i.e. the control over automatically elicited approach and avoidance actions.

Forty human male participants performed a social approach-avoidance task, in which they approached or avoided visually displayed emotional faces (happy or angry) by pulling or pushing a joystick. Approaching angry and avoiding happy faces (incongruent condition) requires rapid application of cognitive control to override prepotent habitual action tendencies to approach appetitive and to avoid aversive situations. In the time window prior to response delivery, trial-by-trial variations in aPFC theta-band power (6 Hz) predicted reaction time increases during emotional control, and were inversely related to beta-band power (14-22 Hz) over parieto-frontal cortex. In sensorimotor areas contralateral to the moving hand, pre-movement gamma-band rhythms (60-90 Hz) were stronger during incongruent than congruent trials, with power increases phase-locked to peaks of the aPFC theta-band oscillations.

These findings define a mechanistic relation between cortical areas involved in implementing rapid control over human social-emotional behavior. The aPFC may bias neural processing towards rule-driven actions and away from automatic emotional tendencies by coordinating tonic disinhibition and phasic enhancement of parieto-frontal circuits involved in action selection.

Significance statement

Being able to control social-emotional behavior is crucial for successful participation in society, as is illustrated by the severe social and occupational difficulties experienced by people suffering from social motivational disorders, such as social anxiety. In this study, we show that theta-band oscillations in the aPFC, which are thought to provide temporal organization for neural firing during communication between distant brain areas, facilitate this control by linking aPFC to parieto-frontal beta-band and sensorimotor gamma-band oscillations involved in action selection. These results contribute to a mechanistic understanding of cognitive control over automatic social-emotional action, and point to frontal theta-band oscillations as a possible target of rhythmic neurostimulation techniques during treatments of social anxiety.

Introduction

81

82

83

84

85

86

87

88

89

90

91

92

93

94

95

96

97

98

99

100

101

102

103

104

105

106

Human cooperative social environment relies on our ability to control social-emotional behavior (Hare, 2017). The importance of this ability is illustrated by conditions in which this control fails. For instance, in social anxiety disorder, persistent avoidance of social interactions causes impairment in social and occupational functioning (Clark and Wells, 1995; Craske and Stein, 2016). Social-emotional disorders also illustrate how regulating social-emotional behavior requires more than suppressing automatic emotional action tendencies. In fact, social-emotional regulation is an action selection feat, involving the selection of adequate behaviors from numerous potential strategies, while anticipating the consequences of those behaviors in other agents. For example, in a job-interview, applicants might make it more likely to get the job when they overcome their tendency to avoid the test and dare to approach when asked who will present first. These emotionally-laden counterfactual computations are thought to be implemented by the anterior prefrontal cortex (aPFC; Daw et al., 2006; Boorman et al., 2009; Volman et al., 2013), a region also known to influence downstream neural activity in the amygdala and posterior parietal cortex (PPC) during emotional action control (Mars et al., 2011; Volman et al., 2011a, 2013, 2016). However, the neural mechanisms that support social-emotional regulation across this network remain unclear. In this study, we use neural oscillations as a metric for understanding how aPFC rapidly selects and implements alternative courses of action over prepotent habitual social-emotional behaviors.

Recent studies have shown that implementation of prefrontal control is often rhythmic, transferring information between regions through entrainment of neural oscillations (Helfrich and Knight, 2016). aPFC neurons tend to phase-lock their spiking and gamma-band firing to the thetaband rhythm (4-8 Hz) (Ardid et al., 2015; Voytek et al., 2015). Frontal theta-band oscillations have been consistently involved in control over motivational behavior (Cavanagh and Frank, 2014; Cooper et al., 2015), including control over state-induced affective behavioral biases (Cavanagh et al., 2013) and feedback-related control in exploration behavior (Cavanagh et al., 2011). Theta-band oscillations might support emotional control by temporally orchestrating release of neurons from inhibition, thus

creating overlapping periods of excitability across the cerebral network involved in social-emotional regulation (Colgin, 2013; Lisman and Jensen, 2013; Volman et al., 2013). Human aPFC has extensive anatomical connections with portions of the PPC (Mars et al., 2011; Neubert et al., 2014), and aPFC-PPC effective connectivity relies on theta-band rhythm modulations (Phillips et al., 2013; Karalis et al., 2016). Here we test whether social-emotional action tendencies are controlled through theta-band oscillations. We explore the dynamics of interactions between theta-band oscillations in aPFC and the beta/gamma rhythms produced by posterior areas during action selection.

We measured neural activity in forty human participants using magnetoencephalography (MEG), while they performed a social approach-avoidance (AA) task. In this task, participants approach or avoid visually-displayed emotional faces by pulling or pushing a joystick, respectively. Approaching angry and avoiding happy faces requires implementing rapid control to override automatic tendencies to approach appetitive and avoid aversive situations. This complex form of control operates on the interaction between the emotional valence of percepts and actions, and it is modulated by social psychopathologies and socially-relevant hormones (Heuer et al., 2007; von Borries et al., 2012; Radke et al., 2013, 2017; Enter et al., 2016).

Previous fMRI studies have shown that during affect-incongruent trials, aPFC and PPC activity is increased, and amygdala activity decreased, suggesting that the aPFC exerts control over social-emotional actions, possibly by interacting with PPC to assist in action selection (Rowe et al., 2008; Volman et al., 2011a). Building on those fMRI and electrophysiological observations, we predict that the emotional control evoked during incongruent trials will result in stronger theta-band power in aPFC. We also explore whether theta-band oscillations over aPFC are coupled to rhythms involved in action selection, i.e. beta- and gamma-band rhythms over parieto-frontal areas (De Lange et al., 2008; Jenkinson and Brown, 2011; Brinkman et al., 2014; Voytek et al., 2015).

Materials and Methods

Participants

Forty-five undergraduate students from the Radboud University took part in the experiment. Five participants did not complete the experiment, with three participants failing to follow task instructions (>30% error trials), and two participants showing substantial noise in the MEG data. Forty participants were considered for analyses (mean age: 23.5, sd: 2.8, range: 18-33 years). All participants signed an informed consent prior to the study and were compensated with monetary reward or research credits. Before inclusion, participants were screened for epilepsy and history of mental illness. All participants were males, right handed and had normal or corrected-to-normal vision. The study was approved by the local ethical committee (CMO:2014/288).

Materials and apparatus

The task was programmed using Presentation software version 16.4 (neurobs.com; RRID:SCR_002521). Stimuli were presented using a PROPixx beamer with a refresh rate of 120 Hz and a resolution of 1920:1080. MEG was acquired using a whole brain CTF-275 system with axial gradiometers. Data were sampled at 1200 Hz after a 300 Hz lowpass filter was applied. Four sensors (MLF62, MLC32, MLC11 & MRF66) were permanently disabled due to high noise. The helmet was set at 15° and the participants were seated 80 cm from the screen. Head location was measured using localization coils in both ear canals and on the nasion and was continuously monitored using online head localization software (Stolk et al., 2013). In case of large deviations from the initial head position (+5 mm) we paused the experiment and instructed the subject to move back to the original position. During the task, participants responded using a customized Fiber Optic Joystick (fORP design), that was calibrated for each participant prior to the experiment. A displacement of 20% away from the center in the sagittal plane was taken as a response.

Participants performed an approach-avoidance (AA) task which has been used in several previous studies (e.g. Volman et al., 2011), and was adapted for MEG; figure 1A. Trials started with the presentation of a white fixation cross presented in the center of a black screen for 1000 ms. After fixation, a face was presented for 100 ms, after which the subject had 2000 ms to respond by pushing the joystick away, or pulling it towards themselves. Participants received written instructions on screen before each block of 12 trials, in which they were instructed to push the joystick towards or away from themselves for happy or angry faces respectively (congruent block), or towards/away from themselves for angry/happy faces (incongruent block). These response rules alternated each block. The task consisted of 16 blocks, yielding 196 trials in total. Stimuli consisted of equiluminant faces that were presented at the center of the screen at a visual angle of 4.3 by 6.4 degrees. In contrast to cognitive control tasks involving conflict on the stimulus level, such as emotional Stroop tasks -typically implicating anterior cingulate cortex-, conflict between emotional percepts and emotional actions such as mapped by the AAT is typically processed by higher order brain regions such as the aPFC (Volman et al., 2011a).

High-resolution anatomical MRI images were acquired with a single-shot MPRAGE sequence (acceleration factor 2 with GRAPPA method, TR 2400ms/TE2.13ms, effective voxel size 1 x 1 x 1mm, 176 sagittal slices, distance factor 50%, flip angle 8 degrees, orientation A >> P, FoV 256mm). To align structural MRI to MEG we provided the participants with vitamin-E capsules in the ears, on the same locations as the localizer coils in the MEG system.

Procedure

Upon arrival, participants received verbal task instructions before changing into non-magnetic clothing. Prior to the experiment participants provided a saliva sample, enabling the quantification of hormone levels for other research purposes. Once in the scanner, participants performed a practice session containing 4 blocks of 8 trials each, using faces of different identity from those displayed in the main experiment. Following the main session of the AA task, participants

provided a second saliva sample and completed the State Trait Anxiety Inventory (Spielberger et al., 1970). Structural MRI was acquired in a separate session where participants also performed the AA task using fMRI. fMRI and hormonal data are not reported here.

Behavioral analysis

Reaction time analyses were performed on correct responses only. We removed trials in which the reaction time exceeded a threshold of three standard deviations above or below the mean reaction time of the subject for each condition separately (1.6 % of trials). Congruency effects in reaction times and error rates were computed by subtracting congruent from incongruent trials.

MEG preprocessing

MEG analyses were performed using Matlab2015a (the Mathworks; RRID:SCR_001622), Fieldtrip toolbox (Oostenveld et al., 2011) and custom written analysis scripts. After epoching the data into trials ranging from -3 s before, until 1 s after response, we removed the third order gradient. The trials were detrended and demeaned in order to remove slow drifts and non-zero DC offset, and filtered using a discrete Fourier transform (DFT) filter to remove the 50 Hz line noise and 100 and 150 Hz harmonics. Next, we performed manual trial rejection to remove trials with large deviations or artifacts. Independent component analysis (Makeig et al., 1996) was performed to remove components that contained sources of noise (e.g. heartbeat, eye-blink, joystick artifacts). After this step, all trials were visually inspected to remove any trial still containing large amounts of noise. For the sensor-level analysis, we interpolated sensors that were missing due to noise removal using a weighted average of neighboring sensors; for some sensors (N=8) this was not possible due to removal of too many neighbors. Sensor level analyses were performed on 263 sensors.

Spectral Analysis

To facilitate interpretation of the topographical distribution of signal resulting from the CTF axial gradiometers, we calculated spectral power for the horizontal and vertical components of the

estimated planar gradient on each sensor location, which we then summed (Bastiaansen and Knösche, 2000). This representation of the data ensures that power of a source is strongest just above that source (Hämäläinen et al., 1993).

Time-frequency representations (TFR) of power were estimated in two steps. For frequencies below 40 Hz, we used Short-time Fourier transform with sliding windows of 500 ms, multiplied with a Hanning taper and moving in steps of 50 ms. The frequency resolution was 2 Hz. We pre-specified 6 Hz as theta-band and 14-22 Hz as beta-band activity. Theta-band definition was based on a-priori expectations (Phillips et al., 2013; Cavanagh and Frank, 2014; Cooper et al., 2015; Karalis et al., 2016). Beta-band definition was based on the congruency effect observed over all sensors. For frequencies above 40 Hz (gamma-band; 40-130 Hz), we used three orthogonal Slepian tapers and sliding time windows of 200 ms (moving in steps of 50 ms), creating frequency smoothing of approximately 10 Hz (frequency resolution of 10 Hz; Percival and Walden, 1993). In the gamma-band analyses, we identified changes in power evoked before response [-1000 until 0 ms], as compared to a baseline period occurring before stimulus presentation (average of -800 until -500 ms). This procedure increased statistical power by narrowing the frequency search space. The frequency band showing increased power (60-90 Hz) was used in further (orthogonal) comparisons between conditions. With the exception of single-trial analyses, all analyses were focused on the contrast between incongruent and congruent conditions.

Source analyses

Congruency effects were localized using DICS beamforming (Groß et al., 2001). We computed a single-shell head model (Nolte, 2003) for each subject using anatomical MRI. Next, we warped the individual MRI images to a template grid in MNI space (spatial resolution of 8 mm). To reconstruct activity in the interval 0.5 s prior to response delivery (period of action selection, see results), we used a Hanning taper followed by a Fourier transform centered at 6 Hz; and three orthogonal Slepian tapers for beta-band (center frequency 18 Hz) and gamma-band (center frequency 75 Hz). Slepian

tapers result in more smoothing in the frequency domain and allowed us to reconstruct activity in a wider frequency range. A common spatial filter was created for each frequency based on all trials. This filter was consequently applied to congruent and incongruent trials separately. We computed relative change in power for incongruent versus congruent (incongruent - congruent) / (incongruent + congruent) to assess differences between conditions. Region labeling was done based on the Harvard-Oxford atlas implemented in FSL (https://fsl.fmrib.ox.ac.uk/fsl/fslwiki/; RRID:SCR_002823).

Spatial filters applied to ROIs

To assess whether gamma-band power is linked to theta-band phase we constructed three spatial filters using linearly constrained minimum variance (LCMV) beamforming. Peak locations for the phase-amplitude analyses were defined based on the peak grid-point resulting from the group level brain-behavior correlation analysis for the theta-band [aPFC; MNI: 40 48 -6], and the group level gamma-band congruency effect; left Postcentral Gyrus [-28 -32 64] and right Parietal Superior Lobule/Postcentral Gyrus [28 -42 70]. These filters were applied to the MEG data after which the dipole direction containing most variance was extracted.

Brain-behavior correlations

The source-reconstructed neural congruency-effects in theta- and beta-band power were correlated with condition differences in reaction time (behavioral congruency-effect). We calculated the correlation between the behavioral and the neural congruency-effects for each grid-point after which we used Fisher's z transform to convert Spearman's r values into z values.

Trial-by-trial estimates [-0.5 s until response] of aPFC theta-band power were obtained from aPFC peak grid-point resulting from the group brain-behavior correlation (centered at [40 48 -6]).

Trial-by-trial estimates of parieto-frontal beta-band power were obtained from a precentral grid-point (centered at [50 -10 36]), resulting from the group level brain-behavior correlation. For each subject, we set up a multiple regression model. First, we used trial-by-trial estimates of theta-band

power (aPFC), beta-band power (precentral), and their interaction (theta_{aPFC}*beta_{precentral}) as predictors of the timeseries of reaction times, separately for congruent and incongruent trials. The regressors were z-scored within each condition, and regression parameters were estimated for each condition and participant separately using robust regression (Matlab function *robustfit*).

Standardized beta values for each subject were used in a second-level analysis testing whether trial-by-trial aPFC theta- and precentral beta-power better accounted for reaction time variance during incongruent than during congruent trials (one-sided dependent-sample t-tests in SPSS, IBM SPSS statistics; RRID:SCR_002865), and whether those regression effects were different from zero (one sample t-tests). In this approach single-trial estimates of power are regressed against single-trial reaction times separately for each condition, a procedure that is orthogonal to the group-level correlation between behavioral-congruency and congruency in theta- and beta-band power.

Connectivity analysis

To assess whether aPFC influences downstream areas by influencing beta-band activity we correlated condition differences in theta-band power extracted from aPFC [MNI: 40 48 -6] with whole brain condition differences in beta-band power. Spearman's *r* values were transformed to *z* values using Fisher's transform.

For theta-gamma coupling we decomposed a spatial filter applied to the aPFC [MNI: 40.48-6] into 6.42 complex signal using STFFT with a 500 ms window tapered with a Hanning filter, moving in steps of 1 ms, after which the peak times between -0.5 s and response were extracted. Next, we time-locked the remaining reconstructed time series (which were extracted from peak locations in the gamma-band condition difference) around each theta-band peak time point. From this (theta peak-locked) signal we extracted gamma-band [40-130~Hz] power by performing STFFT tapered with a Hanning window containing 6 cycles per frequency band (dT = 6/f) and moving in steps of 10 ms. We computed relative change in TFR between conditions for the phase-locked gamma-band power. We tested whether the gamma-band condition difference changed as a function of the phase

of the theta-band extracted from aPFC, an approach which is orthogonal to testing for a difference between the experimental conditions. For interpretational purposes, we also computed the event related field (ERF) of the phase-locked signal from the aPFC to show the underlying theta-band waveform shape.

Statistical analyses

Statistical analyses on the sensor and source level consisted of cluster-based nonparametric permutation tests (Maris and Oostenveld, 2007). This procedure ensures correction for multiple comparisons over time, sensors (or grid points) and frequencies whilst also taking into account the dependency in the data by clustering neighboring points showing the same effect. As test statistics we used t-values on the sensor level data, z-values (fisher transformed *r* values) for brain behavior correlations and theta-beta connectivity, and relative change (incongruent - congruent) / (congruent + incongruent) for the theta-gamma coupling. Unless stated otherwise, the reported p-values refer to cluster-corrected statistics.

Results

Behavioral costs of control over social-emotional action

Reaction times were longer for incongruent (M = 722 ms, sd = 176) as compared to congruent trials (M = 680 ms, sd = 147) [t(39) = -4.33, p <.001. figure 1B; effect size d = .26, calculated as (M1-M2) / sd_{pooled}]. In addition, we found higher accuracy levels for affect-congruent (M = 95.4%, sd = 4) versus incongruent trials (M = 92.3%, sd = 6.5) [t(39) = 3.07, p = .004, d = .57]. These results illustrate that the task is effective in inducing behavioral costs when participants need to override their emotional action tendencies.

297 {Insert figure 1}

aPFC theta-band power increases during emotional-action control

As detailed in the Introduction, we hypothesized that frontal theta-band activity would be involved in control over social-emotional action tendencies. We found stronger theta-band power over anterior sensors before response, during control of automatic emotional actions (i.e. incongruent vs congruent trials; center-frequency: 6 Hz, figure 2A, B). This congruency-effect effect is statistically significant between 350 ms and 100 ms (maximum difference at 200 ms) before response initiation, when controlling for multiple comparisons over sensors (N = 66; ROI on all anterior channels) and time points, p = .016; figure 2A, C. Reconstructing the source locations of this difference showed increases of theta-band activity for incongruent trials with local maxima at right Frontal Pole (aPFC)/Superior Frontal Gyrus [20 40 50], Frontal Pole [26 70 8] and Frontal Orbital Cortex [12 24 -24], figure 2D, with strongest theta-band increases in before response ([20 40 50]; figure 2E).

To localize theta-band activity that is relevant for behavior, we correlated condition differences in theta-band power -0.5 s before- until response in each grid-point with reaction time effects, over participants. ROI analysis on all frontal areas yielded a cluster of activity where the theta-band congruency-effect correlated positively with reaction time congruency-effect (figure 2F, G), $r_{(38)} = .52$, p = .0007 at peak grid point and $r_{(38)} = .44$, p = .045 for the whole cluster, corrected for multiple comparisons over grid points. This cluster had two local maxima, at MNI coordinates [40 48 - 6] and [28 30 40], which correspond to right Frontal Pole and Middle Frontal Gyrus/Superior Frontal Gyrus, respectively. This result indicates that those participants that show greater affectincongruency (as indexed by increased reaction-times for incongruent versus congruent trials) also engage aPFC more strongly. Contralateral (left) Frontal Pole/Inferior Frontal Gyrus showed similar correlations (maximum at [-34 36 12]) but this cluster remained below cluster-correction threshold.

Next, we implemented a post-hoc exploratory analysis to examine whether the relation between increased theta-band power and emotional action control holds even on a trial-by-trial basis. Comparing single trial theta-band power derived from aPFC (MNI: [40 48 -6]) using one-sided t-tests confirmed significant differences between conditions for theta-band power: $t_{(39)} = -1.77$, p = 0.043. Theta-band power in the incongruent condition significantly correlated with behavioral performance in the same condition, $t_{(39)} = 2.69$, p = 0.005. This was not the case for the congruent condition $t_{(39)} = -0.29$, p = 0.77. Together these results confirm our hypothesis that theta-band power is a positive predictor of reaction time and show that aPFC is recruited more strongly with increased incongruence, on a subject-by-subject as well as on a trial-by-trial basis.

{Insert figure 2}

Parietal and frontal beta-band activity decreases during emotional-action control

Next, we tested whether increase in theta-band power would be accompanied by parietal beta-band desynchronization. A large cluster of decreased alpha/beta-band power in incongruent versus congruent condition resulted from the whole brain sensor-level analysis (figure 3A, B), with significant condition differences between 600 ms before response until response onset (maximum difference at time 0), p = .0064 (figure 3C), corrected for multiple comparisons over time points, sensors (N=263) and frequencies. Differences were present over most sensors (figure 3B) and ranged from 8 to 26 Hz (figure 3A), with a peak between 12 and 18 Hz. Splitting the observed effect in alpha (8-12 Hz) and beta-band (14-26 Hz; (e.g. De Lange et al., (2008)) showed a significant decrease for beta-band activity [14-26 Hz], p = .0023; [-600 until response], but not for alpha-band [8-12 Hz, p = .0023; I-600 until response], but not for alpha-band Re-12 Hz, p = .0023; I-600 until response et al., 2008; Jenkinson and Brown, 2011; Brinkman et al., 2014). Reconstructing beta-band activity revealed condition differences (i.e. stronger beta-band desynchronization in the incongruent condition) with a maximum in the right Superior

Parietal Lobule/Supramarginal Gyrus [44 -40 56], figure 3D. Time series reconstruction from right Superior Parietal lobule (figure 3E) illustrates the beta-band desynchronization in this area peaks just before response, and suggest a tight temporal relation with the frontal theta-band effect. These results, combined with the aforementioned theta-band results indicate the involvement of aPFC theta-band and PPC beta-band activity during the control over social-emotional action tendencies, in close anatomical correspondence with previous studies on the control over emotional behavior (e.g. Volman et al., 2011a, 2013).

Correlating beta-band power and behavioral congruency differences revealed a large cluster with $r_{(38)} = -.68$, p < .0001 (peak grid point) and $r_{(38)} = -.48$, p < .0001 (whole cluster), over right Precentral/Postcentral Gyrus with local maximum at [48 -2 36]; figure 3F. This correlation indicates that participants with a large behavioral congruency effect show larger suppression in beta-band power; figure 3G. Single trial beta-band power extracted from the peak location [48 -2 36] was significantly correlated with behavioral performance, $t_{(39)} = -3.06$, p = .002 for incongruent, but not for congruent trials; $t_{(39)} = -.137$, p = .45, and also differed significantly between conditions; $t_{(39)} = 1.8$, p = .04. This indicates that beta-band desynchronization over parieto-frontal regions is behaviorally relevant when control over social-emotional actions is implemented.

365 {Insert figure 3}

 ${\it Effective\ connectivity\ between\ aPFC\ and\ parieto-frontal\ areas\ during\ emotional-action\ control}$

As a next step, we tested whether aPFC theta-band activity modulates rhythms involved in action selection. To assess connectivity between aPFC theta-band power and activity in anatomically downstream areas, we correlated the condition difference in aPFC theta-band power (MNI: [40 48 - 6], local maximum of brain-behavior congruency effects, figure 2F,G) with the condition difference in

beta-band power across each brain grid point, on a subject-by-subject basis. Whole brain analysis yielded a significant cluster, $r_{(38)} = -.61$, p < .0001 (peak grid point), $r_{(38)} = -.46$, p = .021 (whole cluster; corrected for multiple comparisons over grid points) over right Precentral Gyrus/Postcentral Gyrus with a local maximum at [50 -10 36], extending anteriorly into the Middle Frontal Gyrus and posteriorly into the Superior Parietal Lobule (figure 4A; B). Contralateral (left) Precentral Gyrus/Postcentral Gyrus showed similar connectivity below whole-brain corrected threshold. This effect indicates that participants with larger increases in aPFC theta-band power during control over social-emotional actions, also show a larger decrease in beta-band power over parieto-frontal areas. These findings suggest functional coupling between those two oscillatory phenomena in those two cortical regions. There were no significant connectivity effects following i) ROI analysis over the parietal cortex, based on Volman 2011a; ii) exploratory correlational analyses with (theta-band) seed grid point at [28 30 40] (Middle Frontal Gyrus/Superior Frontal Gyrus); iii) single trial correlations between aPFC theta-band and beta-band activity from the connectivity peak location [50 -10 36]; or iv) exploratory phase-amplitude coupling between aPFC theta-band phase and precentral beta-band power.

{Insert figure 4}

Gamma-band activity increases during emotional-action control

Given that aPFC theta-band is thought to provide temporal organization to gamma-band activity (Lisman and Jensen, 2013; Voytek et al., 2015), we explored whether controlling emotional action tendencies resulted in changes in gamma-band power. To determine the frequency range of gamma-band activity evoked in these experimental settlings, we first compared gamma-band power evoked before response with gamma-band power during baseline, over all trials. This comparison showed an increase in power between 60 and 90 Hz (mid-gamma range; Buzsáki and Wang, (2012)), localized over central sensors, p = .027 corrected for multiple comparisons over frequencies, time

points and sensors (N=263). Comparing 60-90 Hz gamma-band power between conditions showed stronger power for incongruent than congruent trials over central sensors (figure 5A, B), starting 350 ms before response until 50 ms before response, p = .03 (figure 5C), corrected for multiple comparisons for time points and sensors (N=263). Source reconstruction of gamma-band condition differences showed power increases with local maxima in right Parietal Superior Lobule/Postcentral Gyrus [28 -40 72], left Postcentral Gyrus [-28 -32 64] and left Superior Frontal Gyrus [-12 16 64] (figure 5D), indicating increased engagement of sensorimotor and parietal areas during control over prepotent habitual actions (figure 5E). There was no significant correlation between gamma-band congruency and reaction time congruency effects, $r_{(38)} = .26$, p = .097.

Finally, to explore whether aPFC control over automatic action tenedencies may involve coupling to sensorimotor gamma-oscillations, we explored the presence of phase-amplitude coupling between theta-band phase at aPFC [40 48 -6], and gamma-band power over left Central Sulcus [-28 - 32 64] and right Parietal Superior Lobule/Postcentral Gyrus [28 -42 70]. In the incongruent condition, there was stronger gamma-band power over left Postcentral Gyrus during peaks- but not during throughs of the aPFC theta-band signal; p = .013, p = .015, and p = .025 for the first, second, and third cluster shown in figure 5F (left to right; corrected for multiple comparisons over time points and frequencies). These results indicate that the increased gamma-band power evoked over controlateral sensorimotor cortex during the control of prepotent habitual actions might be guided by long-range communication between aPFC and those sensorimotor areas.

{Insert figure 5}

Discussion

This study explores neurophysiological mechanisms implementing control over social-emotional behavior. We show that the known contributions of aPFC and PPC to the control of social-emotional behavior are implemented through modulations of neural rhythmic activity in the theta-, beta-, and

gamma-band. More precisely, when participants select an affect-incongruent response to emotional faces, theta-band power increases over aPFC. The increase in theta-band power corresponds to decreases in beta-band power over parieto-frontal cortex, and theta phase-locked increases in gamma-band power over sensorimotor areas. Those modulations of neural rhythmic activity, as well as their temporal dynamics, are behaviorally relevant for the control of social-emotional behavior, both between- as well as within-subjects. Trial-by-trial increases in reaction times during incongruent trials are accounted for by increases in theta-band power over aPFC, and decreases in beta-band power over parieto-frontal cortex.

Prefrontal theta-band oscillations during control of social-emotional behavior

Previous work has shown the importance of theta-band oscillations in overcoming motivational action biases in favor of goal-directed behavior (Cavanagh et al., 2013). Those theta-band oscillations, evoked in the context of a pavlovian learning paradigm, emerged from the medial prefrontal cortex (mPFC), a region frequently associated with cognitive control involving action inhibition (Ridderinkhof et al., 2004) and conflict monitoring (Etkin et al., 2006, 2011). Here, we add two novel elements to that knowledge. First, we show that the theta-band rhythm is also involved in the proactive control of social-emotional action tendencies requiring the rapid selection of actions alternative to a prepotent habitual response. This instance of cognitive control operates on the interaction between emotional percepts and action selection, over and above the emotional value of the stimulus or the emotional value of the response alone. Second, the theta-band rhythm supporting this type of cognitive control emerges from the anterior-lateral prefrontal cortex.

The increased theta-band power observed in this study could be an instance of low-frequency modulations of cortical ensembles (Jensen and Mazaheri, 2010), e.g. the frequently observed theta-based coordination of medio-frontal neuronal ensembles during rule-retrieval (Colgin, 2013; Harris and Gordon, 2015). However, the anatomical location and functional characteristics of the theta-band effect suggest a more specific mechanism. Namely, we show that

this theta-band related form of control emerged before response delivery from the aPFC, rather than during feedback-processing from medial frontal sources previously associated with inhibitory control and memory retrieval (Cavanagh et al., 2011; Colgin, 2013; Cavanagh and Frank, 2014). The aPFC, consistently involved in previous fMRI and transcranial magnetic stimulation studies of social-emotional action-control (Kalisch, 2009; Volman et al., 2011a, 2013; Morawetz et al., 2017), has been associated with the ability to control immediate action tendencies while implementing more abstract goals (Burgess et al., 2007; Badre and D'esposito, 2009; Koechlin, 2016; Mansouri et al., 2017), possibly by keeping online non-chosen response options (Boorman et al., 2009). Controlling emotional-action tendencies, differently from emotional Stroop-like tasks involving stimulus-level conflict, requires considering the relative benefit of the unchosen behavioral strategy, before a switch in response set is implemented (Boorman et al., 2009). The timing, anatomical location, and downstream effects of the current theta-band findings fit with the notion that control of emotional action tendencies involves maintenance of counterfactual choices in aPFC.

Parieto-frontal beta-band oscillations during control of social-emotional behavior

Emotional control evoked beta-band desynchronization, localized to parietal cortex. Those features are not compatible with the beta-band synchronization elicited in inferior frontal gyrus (IFG) during action inhibition (Swann et al., 2012; Aron et al., 2014; Bastin et al., 2014; Picazio et al., 2014). Here, beta-band desynchronization likely reflects increased engagement of areas involved in action selection (Brinkman et al., 2014) through release from tonic cortical inhibition (Khanna and Carmena, 2017) and increased cortico-spinal excitability (van Elswijk et al., 2010). This release from inhibition is facilitated by decreases in GABA-ergic tone (Jensen et al., 2005; Yamawaki et al., 2008) and accompanied by increased gamma-band and spiking activity (Spinks et al., 2008; Donner et al., 2009). The parieto-frontal reduction in beta-band power we observe is inversely proportional to trial-bytrial slowing of responses during incongruent trials, and significantly more so than during congruent trials, suggesting that this effect is not a trivial consequence of participants preparing a generic

motor response, nor a systematic effect of task difficulty. In fact, the enhanced tonic beta-band desynchronization observed during incongruent trials might reflect stronger disinhibition of parieto-frontal circuits when competition between multiple possible actions needs to be resolved and a larger neuronal search space needs to be considered (Cisek and Kalaska, 2010; Grent et al., 2013; Brinkman et al., 2014).

Sensorimotor gamma-band oscillations during control over social-emotional behavior

Gamma-band synchronization in the motor system is linked to action preparation and movement selection (Donner et al., 2009; Schoffelen et al., 2011). When multiple response options are available during action preparation, such as during response conflict, increases in gamma-band oscillations are observed. This is often interpreted as simultaneous activation of multiple active response-sets (Gaetz et al., 2013; Grent et al., 2013), with an automatically triggered action competing with an alternative rule-based action. The increase in gamma-band power we observe in the affect-incongruent condition might reflect enhanced coordination of local neuronal ensembles (Buzsáki and Wang, 2012) towards a state space suitable to initiate the correct, rule-based action (De Lange et al., 2008; Churchland et al., 2010; Kaufman et al., 2014), and away from the prepotent habitual action state. The phasic temporal relation between increases in central gamma-band power and peaks in aPFC theta-band oscillations indicates that selection of an alternative action could be implemented through inter-regional communication via phase-dependent modulations of gamma-band rhythms (Lisman and Jensen, 2013; Voytek et al., 2015)

Interpretational issues

It remains to be seen whether the relation between theta-band effects in aPFC, and downstream beta- and gamma-band effects, constitutes a functionally directional and mono-synaptic interaction. It is known that aPFC sits at the top of the prefrontal hierarchy and projects to parietal and premotor areas (Ramnani and Owen, 2004; Miller and D'Esposito, 2005; Voytek et al., 2015; Koechlin, 2016) and the timing of our effects suggests that aPFC might provide top-down regulation.

However, given the lack of precise knowledge on the feedforward versus feedback connectivity of this circuit in humans (Neubert et al., 2014), the directionality of these effects remains elusive. The current findings do not exclude that other regions involved in emotional action selection could mediate inter-regional couplings between aPFC and parieto-frontal cortex, such as the pulvinar (Tyborowska et al., 2016), or the amygdala. The latter has been shown to be down-regulated by aPFC during social-emotional control (Volman et al., 2013), and it is directly influenced by frontal thetaband oscillations during freezing (Karalis et al., 2016).

It could be argued that the theta-band effects we report are generic by-products of increased anxiety during incongruent trials. Previous studies have shown that theta-band activity in mPFC is involved in anxiety and fear behavior (Cavanagh and Shackman, 2015; Harris and Gordon, 2015), with increased theta-band connectivity between hippocampus and mPFC during fear-related inhibition of behavior (Adhikari et al., 2010; Khemka et al., 2017) and increased theta-band activity over mPFC in anxious individuals (Cavanagh and Shackman, 2015). However, the current changes in theta-band power were modulated by variations in performance on a trial-by-trial basis, an effect orthogonal to the systematic changes possibly related to state anxiety.

Source-level changes in aPFC theta-band and fronto-parietal beta-band power arise in the right hemisphere. However, inspection of the data shows sub-threshold effects in the corresponding contralateral regions, suggesting that the right-hemispheric lateralization is a threshold effect of a bilateral process, in line with previous fMRI reports (Volman et al., 2011b, 2013) and with the sensor-level scalp topographies.

The anterior frontal location of the theta-band effect could be an artifact driven by task-related changes in head or eye position. This potential source of between-conditions differences is unlikely to account for the findings. There were identical stimuli and movements across conditions, head movements were monitored with millimeter precision during task performance (Stolk et al., 2013), and ocular artifacts were aggressively removed with ICA.

Phase-amplitude couplings can be inflated by non-sinusoidal oscillations (Lozano-Soldevilla et al., 2016; Cole et al., 2017), sharp transients in the data (Aru et al., 2015), or harmonics of lower frequencies (Jensen et al., 2016). In our case, theta-related harmonics and sharp transients are unlikely to play a role, given that the theta-band and gamma-band signals originate from different cortical regions, with a clear sinusoidal theta-band signal in aPFC. Stronger theta-band power during incongruent trials might lead to more robust phase estimation, but this does not invalidate the presence of increased gamma-band power during peaks of the theta-band oscillation in aPFC.

Conclusion

This study defines neural responses to the problem of controlling human social-emotional behavior. Participants implement rapid changes in their predominant response set and select an alternative course of action by increasing theta-band power over aPFC, tonically decreasing beta-band power over parieto-frontal cortex, and transiently increasing gamma-band power over parietal and sensorimotor cortex through a mechanism phase-locked to prefrontal theta oscillations. These findings provide clear mechanistic targets for interventional studies aimed at enhancing control over social-emotional behaviors in a number of psychopathologies.

537

538

522

523

524

525

526

527

528

529

530

531

532

533

534

535

536

References

- Adhikari A, Topiwala MA, Gordon JA (2010) Synchronized activity between the ventral hippocampus and the medial prefrontal cortex during anxiety. Neuron 65:257–269.
- Ardid S, Vinck M, Kaping D, Marquez S, Everling S, Womelsdorf T (2015) Mapping of functionally
 characterized cell classes onto canonical circuit operations in primate prefrontal cortex. J
 Neurosci 35:2975–2991.
- Aron AR, Robbins TW, Poldrack RA (2014) Inhibition and the right inferior frontal cortex: one decade on. Trends Cogn Sci 18:177–185.
- Aru J, Aru J, Priesemann V, Wibral M, Lana L, Pipa G, Singer W, Vicente R (2015) Untangling crossfrequency coupling in neuroscience. Curr Opin Neurobiol 31:51–61.
- Badre D, D'esposito M (2009) Is the rostro-caudal axis of the frontal lobe hierarchical? Nat Rev
 Neurosci 10:659–669.

| 550 551 | Bastiaansen MCM, Knösche TR (2000) Tangential derivative mapping of axial MEG applied to event-related desynchronization research. Clin Neurophysiol 111:1300–1305. |
|-------------------|---|
| 552 553 554 | Bastin J, Polosan M, Benis D, Goetz L, Bhattacharjee M, Piallat B, Krainik A, Bougerol T, Chabardès S, David O (2014) Inhibitory control and error monitoring by human subthalamic neurons. Transl Psychiatry 4:e439. |
| 555 556 557 | Boorman ED, Behrens TEJ, Woolrich MW, Rushworth MFS (2009) How green is the grass on the other side? Frontopolar cortex and the evidence in favor of alternative courses of action. Neuron 62:733–743. |
| 558 559 | Brinkman L, Stolk A, Dijkerman HC, de Lange FP, Toni I (2014) Distinct roles for alpha-and beta-band oscillations during mental simulation of goal-directed actions. J Neurosci 34:14783–14792. |
| 560 561 | Burgess PW, Dumontheil I, Gilbert SJ (2007) The gateway hypothesis of rostral prefrontal cortex (area 10) function. Trends Cogn Sci 11:290–298. |
| 562 | Buzsáki G, Wang X-J (2012) Mechanisms of gamma oscillations. Annu Rev Neurosci 35:203–225. |
| 563 564 | Cavanagh JF, Eisenberg I, Guitart-Masip M, Huys Q, Frank MJ (2013) Frontal theta overrides pavlovian learning biases. J Neurosci 33:8541–8548. |
| 565 566 | Cavanagh JF, Figueroa CM, Cohen MX, Frank MJ (2011) Frontal theta reflects uncertainty and unexpectedness during exploration and exploitation. Cereb Cortex 22:2575–2586. |
| 567 568 | Cavanagh JF, Frank MJ (2014) Frontal theta as a mechanism for cognitive control. Trends Cogn Sci 18:414–421. |
| 569 570 | Cavanagh JF, Shackman AJ (2015) Frontal midline theta reflects anxiety and cognitive control: meta-analytic evidence. J Physiol 109:3–15. |
| 571 572 | Churchland MM, Cunningham JP, Kaufman MT, Ryu SI, Shenoy K V (2010) Cortical preparatory activity: representation of movement or first cog in a dynamical machine? Neuron 68:387–400. |
| 573 574 | Cisek P, Kalaska JF (2010) Neural mechanisms for interacting with a world full of action choices. Annu Rev Neurosci 33:269–298. |
| 575 576 | Clark DM, Wells A (1995) A cognitive model of social phobia. Soc phobia Diagnosis, assessment, Treat 41:22–23. |
| 577 578 | Cole SR, van der Meij R, Peterson EJ, de Hemptinne C, Starr PA, Voytek B (2017) Nonsinusoidal beta oscillations reflect cortical pathophysiology in Parkinson's disease. J Neurosci 37:4830–4840. |
| 579 | Colgin LL (2013) Mechanisms and functions of theta rhythms. Annu Rev Neurosci 36:295–312. |
| 580 581 582 | Cooper PS, Wong ASW, Fulham WR, Thienel R, Mansfield E, Michie PT, Karayanidis F (2015) Theta frontoparietal connectivity associated with proactive and reactive cognitive control processes. Neuroimage 108:354–363. |
| 583 584 | Craske MG, Stein MB (2016) Anxiety. Lancet 388:3048–3059 Available at: http://www.sciencedirect.com/science/article/pii/S0140673616303816. |
| 585 586 | Daw ND, O'doherty JP, Dayan P, Seymour B, Dolan RJ (2006) Cortical substrates for exploratory decisions in humans. Nature 441:876–879. |
| 507 | Do Lange ED, Jonson O, Rayer M, Toni J (2009) Interactions between posterior gamma and frontal |

| 588 | alpha/beta oscillations during imagined actions. Front Hum Neurosci 2:7. |
|-------------------|---|
| 589 590 | Donner TH, Siegel M, Fries P, Engel AK (2009) Buildup of choice-predictive activity in human motor cortex during perceptual decision making. Curr Biol 19:1581–1585. |
| 591 592 | Enter D, Spinhoven P, Roelofs K (2016) Dare to approach: single dose testosterone administration promotes threat approach in patients with social anxiety disorder. Clin Psychol Sci 4:1073–1079. |
| 593 594 | Etkin A, Egner T, Kalisch R (2011) Emotional processing in anterior cingulate and medial prefrontal cortex. Trends Cogn Sci 15:85–93. |
| 595 596 | Etkin A, Egner T, Peraza DM, Kandel ER, Hirsch J (2006) Resolving emotional conflict: a role for the rostral anterior cingulate cortex in modulating activity in the amygdala. Neuron 51:871–882. |
| 597 598 | Gaetz W, Liu C, Zhu H, Bloy L, Roberts TPL (2013) Evidence for a motor gamma-band network governing response interference. Neuroimage 74:245–253. |
| 599 600 | Grent T, Oostenveld R, Jensen O, Medendorp WP, Praamstra P (2013) Oscillatory dynamics of response competition in human sensorimotor cortex. Neuroimage 83:27–34. |
| 601 602 603 | Groß J, Kujala J, Hämäläinen M, Timmermann L, Schnitzler A, Salmelin R (2001) Dynamic imaging of coherent sources: studying neural interactions in the human brain. Proc Natl Acad Sci 98:694–699. |
| 604 605 606 | Hämäläinen M, Hari R, Ilmoniemi RJ, Knuutila J, Lounasmaa O V (1993) Magnetoencephalography—theory, instrumentation, and applications to noninvasive studies of the working human brain. Rev Mod Phys 65:413. |
| 607 608 | Hare B (2017) Survival of the friendliest: Homo sapiens evolved via selection for prosociality. Annu Rev Psychol 68:155–186. |
| 609 610 | Harris AZ, Gordon JA (2015) Long-range neural synchrony in behavior. Annu Rev Neurosci 38:171–194. |
| 611 612 | Helfrich RF, Knight RT (2016) Oscillatory Dynamics of Prefrontal Cognitive Control. Trends Cogn Sci 20:916–930. |
| 613 614 | Heuer K, Rinck M, Becker ES (2007) Avoidance of emotional facial expressions in social anxiety: The Approach–Avoidance Task. Behav Res Ther 45:2990–3001. |
| 615 616 | Jenkinson N, Brown P (2011) New insights into the relationship between dopamine, beta oscillations and motor function. Trends Neurosci 34:611–618. |
| 617 618 | Jensen O, Goel P, Kopell N, Pohja M, Hari R, Ermentrout B (2005) On the human sensorimotor-cortex beta rhythm: sources and modeling. Neuroimage 26:347–355. |
| 619 620 | Jensen O, Mazaheri A (2010) Shaping functional architecture by oscillatory alpha activity: gating by inhibition. Front Hum Neurosci 4:186. |
| 621 622 623 | Jensen O, Spaak E, Park H (2016) Discriminating Valid from Spurious Indices of Phase-Amplitude Coupling. eNeuro 3:ENEURO.0334-16.2016 Available at: http://www.ncbi.nlm.nih.gov/pmc/articles/PMC5237829/. |
| 624 625 | Kalisch R (2009) The functional neuroanatomy of reappraisal: time matters. Neurosci Biobehav Rev 33:1215–1226. |

| 626 627 628 | Karalis N, Dejean C, Chaudun F, Khoder S, Rozeske RR, Wurtz H, Bagur S, Benchenane K, Sirota A, Courtin J (2016) 4-Hz oscillations synchronize prefrontal-amygdala circuits during fear behavior. Nat Neurosci 19:605–612. |
|---------------------------------|---|
| 629 630 | Kaufman MT, Churchland MM, Ryu SI, Shenoy K V (2014) Cortical activity in the null space: permitting preparation without movement. Nat Neurosci 17:440–448. |
| 631 632 | Khanna P, Carmena JM (2017) Beta band oscillations in motor cortex reflect neural population signals that delay movement onset. Elife 6. |
| 633 634 | Khemka S, Barnes G, Dolan RJ, Bach DR (2017) Dissecting the function of hippocampal oscillations in a human anxiety model. J Neurosci 37:6869–6876. |
| 635 636 | Koechlin E (2016) Prefrontal executive function and adaptive behavior in complex environments. Curr Opin Neurobiol 37:1–6. |
| 637 | Lisman JE, Jensen O (2013) The theta-gamma neural code. Neuron 77:1002–1016. |
| 638 639 640 | Lozano-Soldevilla D, ter Huurne N, Oostenveld R (2016) Neuronal oscillations with non-sinusoidal morphology produce spurious phase-to-amplitude coupling and directionality. Front Comput Neurosci 10. |
| 641 642 | Makeig S, Bell AJ, Jung T-P, Sejnowski TJ (1996) Independent component analysis of electroencephalographic data. Adv Neural Inf Process Syst:145–151. |
| 643 644 | Mansouri FA, Koechlin E, Rosa MGP, Buckley MJ (2017) Managing competing goals-a key role for the frontopolar cortex. Nat Rev Neurosci. |
| 645 646 | Maris E, Oostenveld R (2007) Nonparametric statistical testing of EEG-and MEG-data. J Neurosci Methods 164:177–190. |
| 647 648 649 650 | Mars RB, Jbabdi S, Sallet J, O'Reilly JX, Croxson PL, Olivier E, Noonan MP, Bergmann C, Mitchell AS, Baxter MG (2011) Diffusion-weighted imaging tractography-based parcellation of the human parietal cortex and comparison with human and macaque resting-state functional connectivity. J Neurosci 31:4087–4100. |
| 651 | Miller BT, D'Esposito M (2005) Searching for "the top" in top-down control. Neuron 48:535–538. |
| 652 653 654 655 656 | Morawetz C, Bode S, Derntl B, Heekeren HR (2017) The effect of strategies, goals and stimulus material on the neural mechanisms of emotion regulation: A meta-analysis of fMRI studies. Neurosci Biobehav Rev 72:111–128 Available at: http://www.sciencedirect.com/science/article/pii/S014976341630375X [Accessed June 22, 2017]. |
| 657 658 659 | Neubert F-X, Mars RB, Thomas AG, Sallet J, Rushworth MFS (2014) Comparison of human ventral frontal cortex areas for cognitive control and language with areas in monkey frontal cortex. Neuron 81:700–713. |
| 660 661 662 | Nolte G (2003) The magnetic lead field theorem in the quasi-static approximation and its use for magnetoencephalography forward calculation in realistic volume conductors. Phys Med Biol 48:3637. |
| 663 664 | Oostenveld R, Fries P, Maris E, Schoffelen J-M (2011) FieldTrip: open source software for advanced analysis of MEG, EEG, and invasive electrophysiological data. Comput Intell Neurosci 2011:1. |
| 665 | Percival DB, Walden AT (1993) Spectral analysis for physical applications. cambridge university press. |

| 666 667 668 | Phillips JM, Vinck M, Everling S, Womelsdorf T (2013) A long-range fronto-parietal 5-to 10-Hz network predicts "top-down" controlled guidance in a task-switch paradigm. Cereb Cortex 24:1996–2008. |
|--------------------------|---|
| 669 670 | Picazio S, Veniero D, Ponzo V, Caltagirone C, Gross J, Thut G, Koch G (2014) Prefrontal control over motor cortex cycles at beta frequency during movement inhibition. Curr Biol 24:2940–2945. |
| 671 672 | Radke S, Roelofs K, De Bruijn ERA (2013) Acting on anger: social anxiety modulates approachavoidance tendencies after oxytocin administration. Psychol Sci 24:1573–1578. |
| 673 674 | Radke S, Volman I, Kokal I, Roelofs K, de Bruijn ERA, Toni I (2017) Oxytocin reduces amygdala responses during threat approach. Psychoneuroendocrinology 79:160–166. |
| 675 676 | Ramnani N, Owen AM (2004) Anterior prefrontal cortex: insights into function from anatomy and neuroimaging. Nat Rev Neurosci 5. |
| 677 678 | Ridderinkhof KR, Ullsperger M, Crone EA, Nieuwenhuis S (2004) The role of the medial frontal cortex in cognitive control. Science (80-) 306:443–447. |
| 679 680 681 | Rowe J, Hughes L, Eckstein D, Owen AM (2008) Rule-selection and action-selection have a shared neuroanatomical basis in the human prefrontal and parietal cortex. Cereb Cortex 18:2275–2285. |
| 682 683 | Schoffelen J-M, Poort J, Oostenveld R, Fries P (2011) Selective movement preparation is subserved by selective increases in corticomuscular gamma-band coherence. J Neurosci 31:6750–6758. |
| 684 | Spielberger CD, Gorsuch RL, Lushene RE (1970) Manual for the state-trait anxiety inventory. |
| 685 686 687 | Spinks RL, Kraskov A, Brochier T, Umilta MA, Lemon RN (2008) Selectivity for grasp in local field potential and single neuron activity recorded simultaneously from M1 and F5 in the awake macaque monkey. J Neurosci 28:10961–10971. |
| 688 689 | Stolk A, Todorovic A, Schoffelen J-M, Oostenveld R (2013) Online and offline tools for head movement compensation in MEG. Neuroimage 68:39–48. |
| 690 691 692 693 | Swann NC, Cai W, Conner CR, Pieters TA, Claffey MP, George JS, Aron AR, Tandon N (2012) Roles for the pre-supplementary motor area and the right inferior frontal gyrus in stopping action: electrophysiological responses and functional and structural connectivity. Neuroimage 59:2860–2870. |
| 694 695 | Tyborowska A, Volman I, Smeekens S, Toni I, Roelofs K (2016) Testosterone during puberty shifts emotional control from pulvinar to anterior prefrontal cortex. J Neurosci 36:6156–6164. |
| 696 697 | van Elswijk G, Maij F, Schoffelen J-M, Overeem S, Stegeman DF, Fries P (2010) Corticospinal betaband synchronization entails rhythmic gain modulation. J Neurosci 30:4481–4488. |
| 698 699 | Volman I, Roelofs K, Koch S, Verhagen L, Toni I (2011a) Anterior prefrontal cortex inhibition impairs control over social emotional actions. Curr Biol 21:1766–1770. |
| 700 701 | Volman I, Toni I, Verhagen L, Roelofs K (2011b) Endogenous testosterone modulates prefrontal—amygdala connectivity during social emotional behavior. Cereb Cortex:bhr001. |
| 702 703 704 | Volman I, Verhagen L, den Ouden HEM, Fernández G, Rijpkema M, Franke B, Toni I, Roelofs K (2013) Reduced serotonin transporter availability decreases prefrontal control of the amygdala. J |

| 705 706 707 | Volman I, von Borries AKL, Bulten BH, Verkes RJ, Toni I, Roelofs K (2016) Testosterone modulates altered prefrontal control of emotional actions in psychopathic offenders. ENeuro 3:ENEURO-0107. |
|-------------------|---|
| 708 709 710 | von Borries AKL, Volman I, de Bruijn ERA, Bulten BH, Verkes RJ, Roelofs K (2012) Psychopaths lack the automatic avoidance of social threat: relation to instrumental aggression. Psychiatry Res 200:761–766. |
| 711 712 713 | Voytek B, Kayser AS, Badre D, Fegen D, Chang EF, Crone NE, Parvizi J, Knight RT, D'esposito M (2015) Oscillatory dynamics coordinating human frontal networks in support of goal maintenance. Nat Neurosci. |
| 714 715 716 | Yamawaki N, Stanford IM, Hall SD, Woodhall GL (2008) Pharmacologically induced and stimulus evoked rhythmic neuronal oscillatory activity in the primary motor cortex in vitro. Neuroscience 151:386–395. |
| 717 | |
| 718 | |
| 719 | Figure Legends |
| 720 | |
| 721 | Figure 1: Approach-avoidance (AA) task and behavioral results. |
| 722 | Panel A shows a schematic representation of the affect-congruent and affect-incongruent conditions |
| 723 | in the AA task. Panel B shows average reaction times for each participant (N=40) and condition. |
| 724 | Responses are slower during incongruent trials. *: $t_{(39)} = -4.33$, $p < .001$. |
| 725 | |
| 726 | Figure 2: Emotional control increases theta-band power in anterior prefrontal cortex. A) time- |
| 727 | frequency plot of between conditions power differences (congruency effect: incongruent – congruent |
| 728 | / congruent + incongruent) averaged over sensors with a significant effect (see panel B). Time 0: |
| 729 | response onset. The dashed box shows the time-frequency interval with a significant congruency |
| 730 | effect [-350 to -100 ms before response; 6 Hz]. B) topographic distribution of sensors with a |
| 731 | significant congruency effect at 6 Hz (marked by stars). C) changes over time in theta-band power (6 |
| 732 | Hz) averaged across significant sensors (see panel B). The epoch with a significant difference between |
| 733 | conditions is marked in grey. D) Cortical distribution of theta-band congruency effects. E) Time series |
| 734 | of 6 Hz activity extracted from right frontal note/superior frontal avrus [20 40 50] E) Cortical |

distribution of correlations between theta-band and behavioral congruency effects, with a significant cluster over aPFC (dashed black circle, MNI coordinates of local maximum: [40 48 -6]). G) correlation between theta-band and behavioral congruency effects. Black dots represent measurements from each participant. Theta-band power changes are extracted from the local maximum in aPFC.

Figure 3: Emotional control decreases beta-band power in parietal and frontal cortex. A) timefrequency plot of between conditions power differences (congruency effect: incongruent – congruent
/ congruent + incongruent) averaged over sensors with a significant effect (see panel B). Time 0:
response onset. The dashed box shows the time-frequency interval with a significant congruency
effect [-600 to 0 ms before response; 14-26 Hz]. B) topographic distribution of sensors with a
significant congruency effect at 14-26 Hz (marked by stars). C) changes over time in beta-band power
(14-26 Hz) averaged across significant sensors (see panel B). The epoch with a significant difference
between conditions is marked in grey. D) Cortical distribution of beta-band congruency effects (center
frequency 18 Hz). E) Time series of 18 Hz activity extracted from Superior Parietal Lobule [44 -40 56].
F) Cortical distribution of correlations between beta-band (18 Hz) and behavioral congruency effects,
with a significant cluster over right precentral gyrus (MNI coordinates of local maximum: [48 -2 36]).
G) correlation between beta-band and behavioral congruency effects. Black dots represent
measurements from each participant. Beta-band power changes are extracted from the right
precentral maximum.

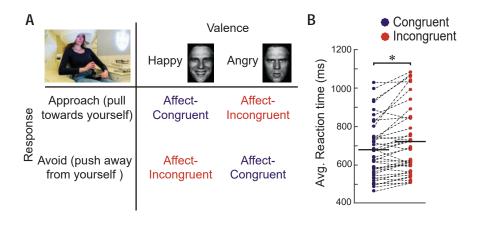
Figure 4: Emotional control increases connectivity between aPFC and fronto-parietal areas. A)

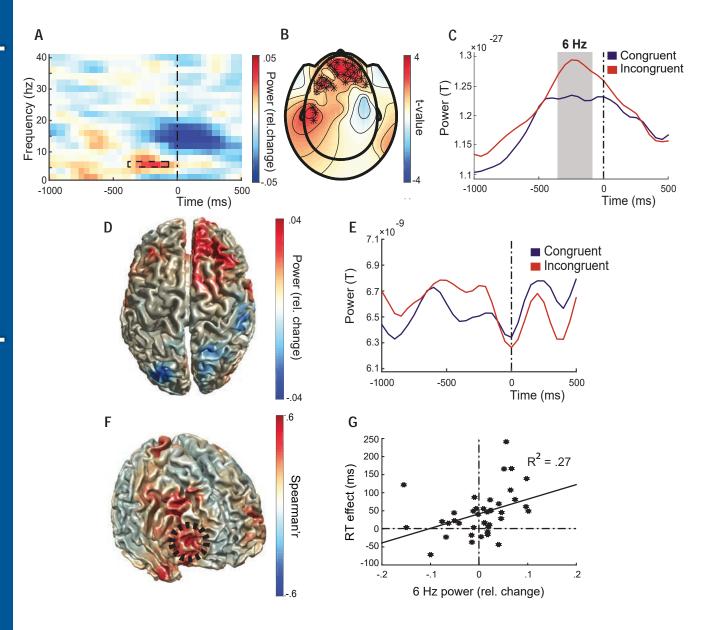
Cortical distribution (uncorrected for multiple comparisons) of correlations between beta-band congruency effects and theta-band congruency effects extracted from aPFC (in red, from Figure 2E).

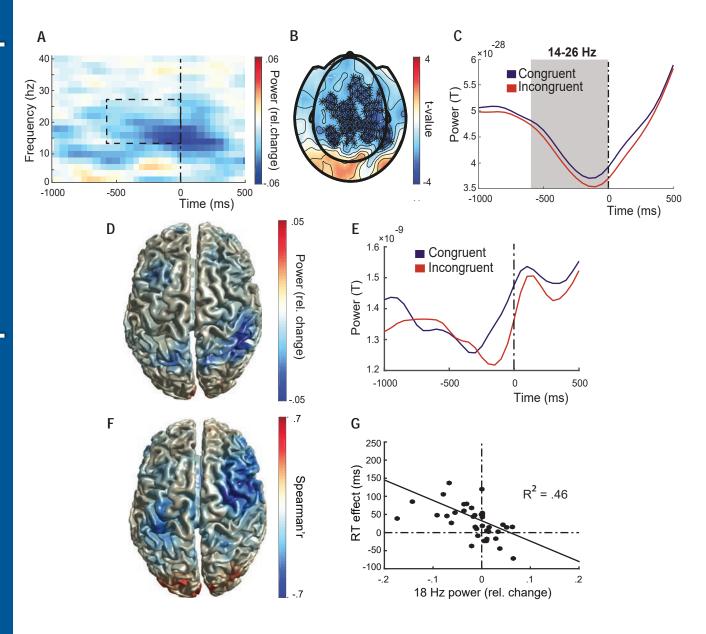
The cluster over the right precentral gyrus (MNI coordinates of local maximum: [50 -10 36]) is significant. B) correlation between aPFC theta-band and precentral beta-band congruency effects.

Black dots represent measurements from each participant. Beta-band power changes are extracted from the right precentral maximum.

Figure 5: Emotional control increases gamma-band power in parietal and frontal cortex during peaks of theta-band oscillations in aPFC. A) Time-frequency plot of between conditions power differences (congruency effect: incongruent – congruent / congruent + incongruent) averaged over sensors with a significant effect (see panel B). Time 0: response onset. The dashed box shows the time-frequency interval with a significant congruency effect [-350 to -50 ms before response; 60-90 Hz]. B) topographic distribution of sensors with a significant congruency effect at 60-90 Hz (marked by stars). C) changes over time in gamma-band power (60-90 Hz) averaged across significant sensors (see panel B). D) Cortical distribution of relative gamma-band congruency effects, with a significant cluster around the left central sulcus [-28 -32 64]. E) Time series of 60-90 Hz activity extracted from left central sulcus [-28 -32 64]. F) Time-frequency plot of gamma-band power congruency effects extracted from the local maximum in the left central sulcus (panel F); phase-locked to the aPFC thetaband signal before response. Contours are drawn around significant clusters where power is stronger in incongruent versus congruent trials. G) event related field of the theta-band signal extracted from aPFC.







Α

